



Seed run-off in an MHD air preheater  
by Rosanne Marie Nash

A thesis submitted in partial fulfillment of the requirements for the degree of MASTER OF SCIENCE  
in MECHANICAL ENGINEERING

Montana State University

© Copyright by Rosanne Marie Nash (1978)

Abstract:

Potassium sulphate (seed) flow and buildup on a tube wall of a cored brick regenerative air preheater was modeled using an adaptation of a previously developed slag flow computer model. The slag and seed flow problems will be encountered in air preheaters used in proposed open cycle magnetohydrodynamic (MHD) power generation. Two cases of flow which simulated experimental conditions of two runs on the Flui-Dyne Engineering Corporation experimental air preheater were modeled. Comparison of analytical and experimental results showed that the model can reasonably predict the occurrence of flow restrictions in the tube due to seed buildup but the magnitudes of the restrictions cannot be predicted due to limitations of the model.

STATEMENT OF PERMISSION TO COPY

In presenting this thesis in partial fulfillment of the requirements for an advanced degree at Montana State University, I agree that the Library shall make it freely available for inspection. I further agree that permission for extensive copying of this thesis for scholarly purposes may be granted by my major professor, or, in his absence, by the Director of Libraries. It is understood that any copying or publication of this thesis for financial gain shall not be allowed without my written permission.

Signature Rosanne M. Nash

Date 10/2/78

SEED RUN-OFF IN AN MHD AIR PREHEATER

by

ROSANNE MARIE NASH

A thesis submitted in partial fulfillment  
of the requirements for the degree

of

MASTER OF SCIENCE

in

MECHANICAL ENGINEERING

Approved:

H. W. Thomas

Chairperson, Graduate Committee

Dennis O. Blackletter

Head, Major Department

Henry L. Parsons

Graduate Dean

MONTANA STATE UNIVERSITY  
Bozeman, Montana

October, 1978

ACKNOWLEDGEMENTS

The author would like to thank Dr. H. W. Townes for his help and guidance in preparing this thesis. The author would also like to thank her husband, Rusty, for his support and encouragement.

TABLE OF CONTENTS

|                                                                                                                                                  | <u>Page</u> |
|--------------------------------------------------------------------------------------------------------------------------------------------------|-------------|
| VITA . . . . .                                                                                                                                   | ii          |
| ACKNOWLEDGEMENTS . . . . .                                                                                                                       | iii         |
| LIST OF TABLES . . . . .                                                                                                                         | v           |
| LIST OF FIGURES . . . . .                                                                                                                        | vi          |
| NOMENCLATURÉ . . . . .                                                                                                                           | vii         |
| ABSTRACT . . . . .                                                                                                                               | ix          |
| CHAPTER I: INTRODUCTION . . . . .                                                                                                                | 1           |
| CHAPTER II: LITERATURE REVIEW . . . . .                                                                                                          | 3           |
| CHAPTER III: THEORY . . . . .                                                                                                                    | 4           |
| CHAPTER IV: RESULTS . . . . .                                                                                                                    | 10          |
| CHAPTER V: CONCLUSIONS . . . . .                                                                                                                 | 31          |
| APPENDIX I: DEVELOPMENT OF THE PARTIAL DIFFERENTIAL EQUATION<br>GOVERNING THE SEED LAYER THICKNESS AND RESULTING<br>STABILITY CRITERIA . . . . . | 32          |
| APPENDIX II: DEVELOPMENT OF RELATIONSHIPS SIMULATING<br>EXPERIMENTAL CONDITIONS . . . . .                                                        | 36          |
| LITERATURE CITED . . . . .                                                                                                                       | 44          |

LIST OF TABLES

|                                            | <u>Page</u> |
|--------------------------------------------|-------------|
| 1. Stable Case Flow Conditions . . . . .   | 11          |
| 2. Unstable Case Flow Conditions . . . . . | 12          |

## LIST OF FIGURES

|                                                        | <u>Page</u> |
|--------------------------------------------------------|-------------|
| 1. Seed thickness profile . . . . .                    | 14          |
| 2. Seed thickness profile . . . . .                    | 15          |
| 3. Seed thickness profile . . . . .                    | 17          |
| 4. Seed thickness profile . . . . .                    | 18          |
| 5. Seed thickness profile . . . . .                    | 20          |
| 6. Seed thickness profile . . . . .                    | 21          |
| 7. Seed thickness profile . . . . .                    | 23          |
| 8. Seed thickness profile . . . . .                    | 25          |
| 9. Seed thickness profile . . . . .                    | 26          |
| 10. Seed thickness profile . . . . .                   | 27          |
| 11. Seed thickness profile . . . . .                   | 28          |
| 1.1 Axial element of fluid layer . . . . .             | 32          |
| 2.1 Stable case axial temperature profiles . . . . .   | 37          |
| 2.2 Unstable case axial temperature profiles . . . . . | 38          |

## NOMENCLATURE

| <u>Symbol</u> | <u>Description</u>                         |
|---------------|--------------------------------------------|
| A             | Cross-sectional area of flow               |
| BT            | Total blowdown cycle time                  |
| c             | Fluid specific heat                        |
| C             | Circumference of flow tube                 |
| $C_+$         | Weight concentration of seed in gas stream |
| D             | Diameter of flow tube                      |
| f             | Friction factor                            |
| g             | Acceleration due to gravity                |
| k             | Fluid thermal conductivity                 |
| $k_s$         | Equivalent sand grain roughness factor     |
| $k_+$         | Dimensionless particle deposition velocity |
| L             | Length of axial element                    |
| $\dot{m}$     | Seed mass deposition from gas stream       |
| $\dot{m}_a$   | Mass flow rate of gas stream               |
| P             | Local pressure                             |
| r             | Radial position                            |
| Re            | Reynolds number for gas flow               |
| RT            | Total reheat cycle time                    |
| t             | Time                                       |
| T             | Fluid temperature                          |
| Temp          | Wall temperature                           |

| <u>Symbol</u>                   | <u>Description</u>                       |
|---------------------------------|------------------------------------------|
| TK                              | Gas stream temperature                   |
| u                               | Velocity component in axial direction    |
| v                               | Velocity component in radial direction   |
| V                               | Average gas velocity                     |
| $\bar{V}$                       | Mean fluid velocity                      |
| $\forall$                       | Elemental volume                         |
| $\dot{\forall}$                 | Volumetric flow rate                     |
| y                               | Dimension measured from tube wall inward |
| Z                               | Axial position                           |
| $\Delta t$                      | Time step                                |
| $\Delta Z$                      | Axial step                               |
| $\delta$                        | Fluid layer thickness                    |
| $\rho$                          | Fluid density                            |
| $\rho_f$                        | Gas stream density                       |
| $\mu$                           | Dynamic viscosity                        |
| $\tau_g$                        | Surface shear due to gas flow            |
| subscript j denotes axial step  |                                          |
| superscript n denotes time step |                                          |

## ABSTRACT

Potassium sulphate (seed) flow and buildup on a tube wall of a cored brick regenerative air preheater was modeled using an adaptation of a previously developed slag flow computer model. The slag and seed flow problems will be encountered in air preheaters used in proposed open cycle magnetohydrodynamic (MHD) power generation. Two cases of flow which simulated experimental conditions of two runs on the Fluid-Dyne Engineering Corporation experimental air preheater were modeled. Comparison of analytical and experimental results showed that the model can reasonably predict the occurrence of flow restrictions in the tube due to seed buildup but the magnitudes of the restrictions cannot be predicted due to limitations of the model.

## CHAPTER I

### INTRODUCTION

Efficient operation of proposed coal-fired, open-cycle magnetohydrodynamic (MHD) power generating plants will require combustion gas temperatures on the order of  $3000^{\circ}\text{K}$ . A prerequisite for successfully obtaining these temperatures is that the combustion air be preheated prior to the combustion process.

A ceramic fixed-bed regenerative heat exchanger utilizing exhaust gases from the MHD channel to preheat incoming combustion air is currently being considered. A major problem associated with this system involves the corrosive potassium sulphate seed- and coal slag-laden MHD exhaust gases. As the gases cool during the heat up of the heat exchanger matrix, the seed and slag particles will condense and deposit along the ceramic walls. The resulting behavior of the seed/slag layer with respect to flow and growth could be a determining factor in the feasibility of the regenerative heat exchanger system.

Consequently, a significant amount of experimental and analytical research has been carried out in an effort to determine the characteristics of the seed/slag flow. An analytical computer model was developed at Montana State University [Clowes, 1] to predict slag flow and build up on the experimental facility located there. The objective of this thesis has been to adapt that analytical slag flow model to the conditions of the Fluidyne Engineering Corporation experimental heat exchanger and to compare these analytical results with the experimental

results obtained by Fluidyne. The Fluidyne facility tested primarily seed flow and the possibility of using pressure drop measurements as an indicator of seed/slag buildup on passage walls.

## CHAPTER II

### LITERATURE REVIEW

Before seed flow in an MHD air preheater can be adequately modeled, the seed mass deposition rate from the gas stream to the passage walls must be accurately known. Many analytical and experimental studies have attempted to determine the rate of particulate deposition from turbulent flow streams. General theoretical models have been developed by Friedlander and Johnstone [2], Davies [3], and Sande [4]. Experimental studies were done by Friedlander and Johnstone [2], and Liu and Agarwal [5]. Ondo [6] reviewed several of the theoretical models and experimental studies. Ondo's review showed that the theoretical models agreed with experimental results for only limited ranges of deposition rates. Overall, the experimental results had a two-order-of-magnitude variation and the theoretical models had a four-order-of-magnitude variation. This indicates that more theoretical and experimental work needs to be done before seed deposition in an MHD air preheater can be accurately predicted.

Slag flow in an MHD channel has been theoretically modeled by Rosa [7]. Experimental measurements of slag flow and slag properties in a simulated MHD channel have been carried out by Rodgers, Ariessohn and Kruger [8].

Clowes [1] developed a theoretical model for slag flow in an MHD air preheater. In the present work, this model has been modified and used to predict seed flow in an MHD air preheater.

## CHAPTER III

### THEORY

The matrix of a ceramic fixed-bed air preheater consists of a stack of cored bricks which form an array of cylindrical flow passages. A model of the seed flow in a single passage is sufficient as the results may be extended to any number of passages provided they are all operating under the same flow conditions.

The momentum, energy, and continuity equations governing the axisymmetric flow of a layer of constant density fluid down the inside of a vertically oriented cylinder from Clowes [1] are as follows:

Momentum:

$$\rho \left( \frac{\partial u}{\partial t} + u \frac{\partial u}{\partial z} + v \frac{\partial u}{\partial r} \right) = \rho g - \frac{\partial P}{\partial z} + \mu \left( \frac{\partial^2 u}{\partial z^2} + \frac{1}{r} \frac{\partial u}{\partial r} + \frac{\partial^2 u}{\partial r^2} \right) \quad (1)$$
$$+ \frac{\partial \mu}{\partial r} \left( \frac{\partial v}{\partial z} + \frac{\partial u}{\partial r} \right) + 2 \frac{\partial u}{\partial z} \frac{\partial \mu}{\partial z}$$

where  $\rho$  = fluid density,

$u$  = velocity component in axial direction,

$v$  = velocity component in radial direction,

$\mu$  = dynamic viscosity,

$g$  = acceleration due to gravity,

$r$  = radial position,

$z$  = axial position,

$P$  = local pressure, and

$t$  = time.

Energy: (with negligible shear work)

$$\frac{\partial}{\partial z} (\rho c T) + \frac{1}{r} \frac{\partial}{\partial r} (r v c \rho T) - \frac{\partial}{\partial z} \left( k \frac{\partial T}{\partial z} \right) - \frac{1}{r} \frac{\partial}{\partial r} \left( r k \frac{\partial T}{\partial r} \right) + \rho c \frac{\partial T}{\partial t} = 0 \quad (2)$$

where  $T$  = fluid temperature,

$c$  = fluid specific heat, and

$k$  = fluid thermal conductivity.

Continuity:

$$\rho \frac{\partial \dot{V}}{\partial t} = \rho \dot{V}_{in} - \rho \dot{V}_{out} \quad (3)$$

where  $\dot{V}$  = volume, and

$\dot{V}$  = volumetric flow rate.

Clowes [1] determined that the stability criteria limiting the size of axial and time steps are too severe to allow a workable solution of the three coupled equations.

In order to obtain a workable model of slag or seed flow, an additional limitation must be imposed. By constraining the model to apply to a thin fluid layer, the temperature can be considered to be constant radially and equal to the ceramic wall temperature [Clowes, 1]. If the axial temperature variation of the wall is known, the energy equation is no longer needed. Since the viscosity is temperature dependent, it, also, will vary only with axial position.

Using these simplifications and rectangular coordinates, the momentum equation at any one axial position becomes the following relationship for the radial velocity profile [Clowes, 1]:

$$u(y) = \frac{-\rho g}{2\mu_j} y^2 + \frac{(\tau_g)_j + \rho g \delta_j}{\mu_j} y \quad (4)$$

where  $j$  = axial position of calculation,

$\tau_g$  = surface shear stress due to gas flow,

$\delta$  = fluid layer thickness, and

$y$  = dimension measured from the tube wall inward.

In the same way, the expanded continuity equation becomes the following partial differential equation (see Appendix 1 for development):

$$\frac{\dot{m}}{\rho} + \frac{\partial(\delta \bar{V})}{\partial z} = \frac{\partial \delta}{\partial t} \quad (5)$$

where  $\dot{m}$  = seed mass deposition from gas stream,

$\bar{V}$  = seed mean fluid velocity,

$$= \frac{1}{\delta} \int_0^{\delta} u(y) dy, \text{ and}$$

$$= \frac{\tau_g \delta}{2\mu} + \frac{\rho g \delta^2}{3\mu}.$$

Equation 5 can be solved using a backward finite difference with respect to fluid velocity direction (see Appendix 1 for explanation). For fluid flowing down the bed with the zero axial position at the top of the bed, equation 5 is approximated as:

$$\delta_j^{n+1} = \delta_j^n + \Delta t \frac{\dot{m}_j}{\rho} + \frac{\Delta t}{\Delta z} \left( \delta_{j-1}^n \cdot \bar{v}_{j-1}^n - \delta_j^n \cdot \bar{v}_j^n \right) \quad (6)$$

where superscript n denotes time, and  
subscript j denotes axial position, measured from top of bed.

Solution of the thickness finite difference equation and the corresponding mean velocity equation requires knowledge of the ceramic wall temperature, seed viscosity, surface shear due to the gas flow, and seed mass deposition rate at all axial positions and at all times during the flow simulation.

The axial temperature variation can be either a curve fit of experimentally measured values or a curve fit of values calculated with an appropriate analytical heat transfer model. If the temperature also varies with time, the functional dependence with respect to time may be fitted in a similar manner.

The seed viscosity is a function of temperature for which empirical relationships are available.

The surface shear due to gas flow can be approximated using the following rough regime pressure drop relationship, the Colebrook-White friction factor relationship, and the shear stress equation:

$$\frac{P_1}{\rho_1 g} + Z_1 = \frac{P_2}{\rho_2 g} + Z_2 + f \frac{L}{D} \frac{V^2}{2g} \quad (7)$$

where  $P$  = local pressure,  
 $Z$  = axial position,  
 $\gamma$  = specific weight of the gas,  
 $f$  = friction factor,  
 $L$  = length of axial element,  
 $D$  = diameter of flow passage,  
 $V$  = average gas velocity, and  
 $\rho$  = gas density.

$$\frac{1}{\sqrt{f}} = 1.74 - 2 \log_{10} \left[ \frac{2 k_s}{D} + \frac{18.7}{Re\sqrt{f}} \right] \quad (8)$$

where  $k_s$  = equivalent sand grain roughness factor, and  
 $Re$  = Reynold's number for gas flow;

$$\tau = \frac{f}{4} \frac{\rho_f V^2}{2g_c} \quad (9)$$

where  $\rho_f$  = gas stream density.

These equations can be solved at different times at each axial element and the resulting shear values can be fitted to give a relationship for shear variation with axial position and time. Either the total pressure drop across the bed or the equivalent sand grain roughness factor must be a known parameter. This development agrees with a thin seed layer approximation in that it does not take into account possible gas flow variations due to a thick seed layer buildup.

The rate at which seed is being deposited onto the flow passage wall is not an easily measured or calculated value. The experimental work of Liu and Agarwal [5] parallels the conditions of an MHD air preheater better than most of the other experimental deposition studies. Their results also agree well with theoretical models over the middle range of deposition velocities as shown by Ondo [6]. Therefore, a first order approximation of seed mass deposition rate can be made by using an experimental deposition velocity from Liu and Agarwal [5] and considering it not to vary with axial position or time.

The seed thickness can now be determined by dividing the air preheater bed into a number of axial steps and calculating the corresponding thickness and mean velocity at each axial position for one time. Time is then incremented by one step and the axial calculations repeated.

## CHAPTER IV

### RESULTS

Two cases of seed flow were modeled. The flow conditions for the two cases correspond to those encountered in FluidDyne's experimental test 5, listed in Tables 1 and 2. This data was obtained from White [9] and Pearson [10] and was used to develop functional forms of the variations of wall temperature, seed viscosity, shear stress due to gas flow, and seed mass deposition rates (see Appendix 2 for details).

The two test cases are designated as stable and unstable. The stable experimental run showed no change in the pressure drop across the bed with an increasing number of cycles while the unstable experimental run showed an increasing pressure drop across the bed with increasing number of cycles. The air preheater bed was found to have significant seed deposition within its flow passages after the unstable experimental run. For both cases the tube diameter was 19.1 mm and the tube length (bed length) was 5.182 m. The seed material used was potassium sulphate.

The term "reheat" refers to the air preheater operational phase in which the bed is being heated by the hot exhaust gases. The term "blow-down" refers to the operational phase in which the precombustion air is being heated by the hot bed. A "cycle" is a combined reheat and blow-down phase.

TABLE 1.--Stable Case Flow Conditions

## Bed Geometry:

Bed Length = 5.182 m  
Number of flow holes = 30  
Diameter of flow holes = 19.1 mm

## Flow Times:

Reheat cycle time = 60 min.  
Blowdown cycle time = 30 min.  
Total run time = 30 hr. 35 min.  
Number of cycles = 20

## Reheat Cycle:

Total gas mass flow rate = 0.0998 kg/sec  
Inlet weight concentration of seed in gas = 2.53%  
Maximum top temperature = 1846°K  
Maximum bottom temperature = 1386°K  
Inlet pressure = 103,422 Pa  
Pressure drop across the bed = 6216 Pa

## Blowdown Cycle:

Total air mass flow rate = 0.1066 kg/sec  
Minimum top temperature = 1630°K  
Minimum bottom temperature = 1188°K  
Inlet pressure = 103,422 Pa  
Pressure drop across the bed = 5221 Pa

## Seed Material - Potassium Sulphate:

Density = 2660 kg/m<sup>3</sup>  
Solidification temperature = 1344°K

TABLE 2.--Unstable Case Flow Conditions

## Bed Geometry:

Bed length = 5.182 m  
Number of flow holes = 30  
Diameter of flow holes = 19.1 mm

## Flow Times:

Reheat cycle time = 30 min.  
Blowdown cycle time = 30 min.  
Total run time = 5 hr. 20 min.  
Number of cycles = 5

## Reheat Cycle:

Total gas mass flow rate = 0.0921 kg/sec  
Inlet weight concentration of seed in gas = 2.74%  
Maximum top temperature = 1715°K  
Maximum bottom temperature = 1289°K  
Inlet pressure = 103,422 Pa  
Pressure drop across the bed = 6987 → 9523 Pa

## Blowdown Cycle:

Total air mass flow rate = 0.0809 kg/sec  
Minimum top temperature = 1522°K  
Minimum bottom temperature = 1105°K  
Inlet pressure = 103,422 Pa  
Pressure drop across the bed = 3580 → 4202 Pa

## Seed Material - Potassium Sulphate:

Density = 2660 kg/m<sup>3</sup>  
Solidification temperature = 1344°K

The major difference in the flow conditions between the two cases is the stable case reheat phase of 60 minutes compared to the unstable case reheat phase of 30 minutes. The result of the longer reheat in the stable case is a higher overall maximum wall temperature profile. By the end of the stable case reheat phase the entire bed length has temperatures above 1344°K, which is the solidification temperature for potassium sulphate.

The results of the two case runs of the seed flow model are shown in Figures 2 through 7. All plots are of the seed thickness profile vs. a dimensionless bed length.

Figure 1 shows the seed thickness profile 1200 seconds into the first 3600 second reheat phase of the stable case. The maximum wall layer thickness is 0.252 mm which occurs at a dimensionless axial position of 0.675. This buildup occurs at the point where the wall temperature falls below the solidification temperature of the seed. Above this point, the deposited seed is flowing down the bed and below this point there is no flow as the deposition is considered to be in the solid phase.

Figure 2 again shows the wall layer thickness profile at 1200 seconds into the first 3600 second reheat of the stable case. This plot is on an expanded horizontal scale to show in greater detail the thin seed layers above and below the seed solidification point. The maximum thickness at the point of solidification extends beyond the scale of the

STABLE CASE  
MINIMUM DEPOSITION RATE  
1200 SECONDS INTO FIRST REHEAT

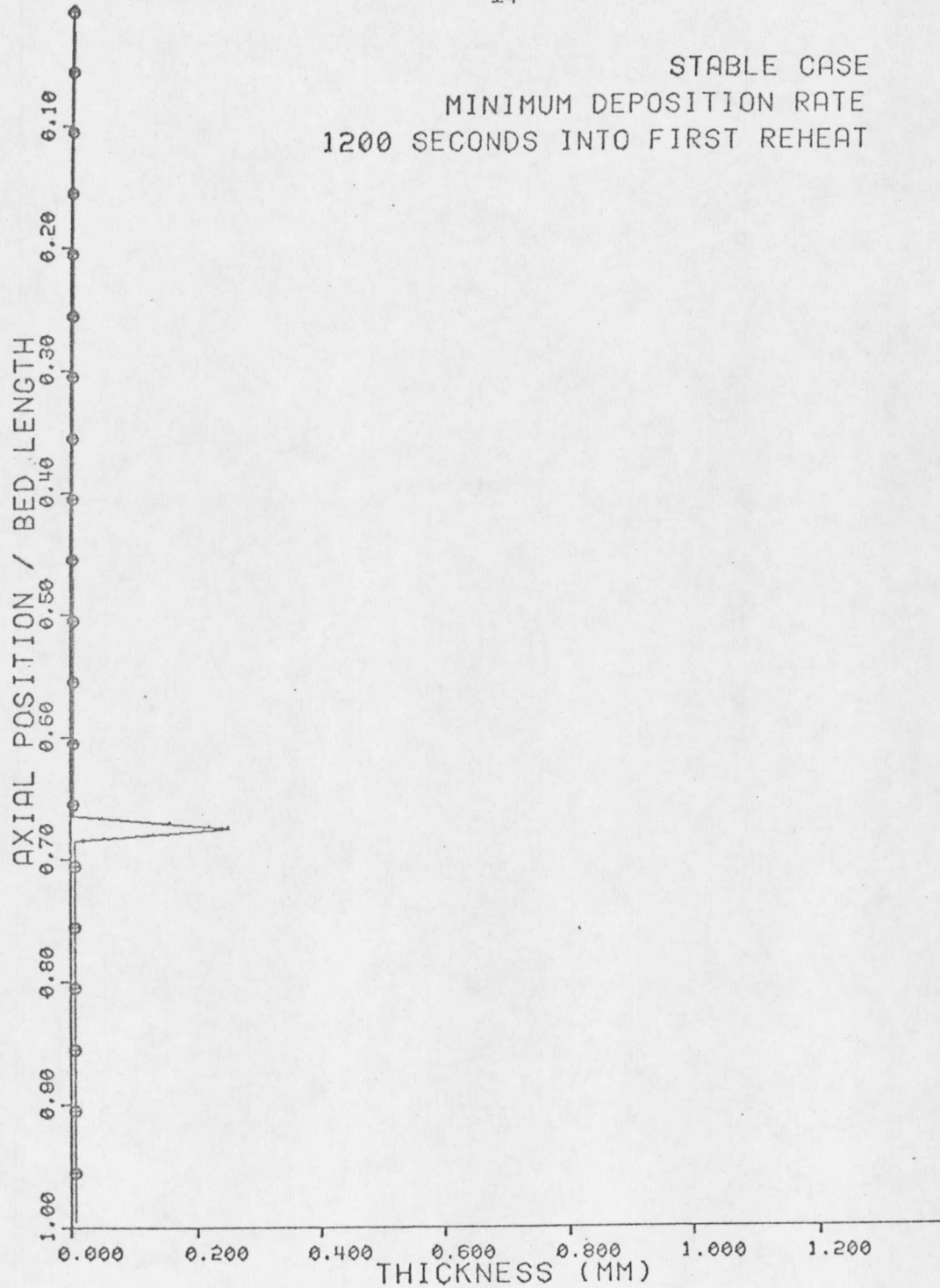


Figure 1.--Seed thickness profile

STABLE CASE  
MINIMUM DEPOSITION RATE  
1200 SECONDS INTO FIRST REHEAT

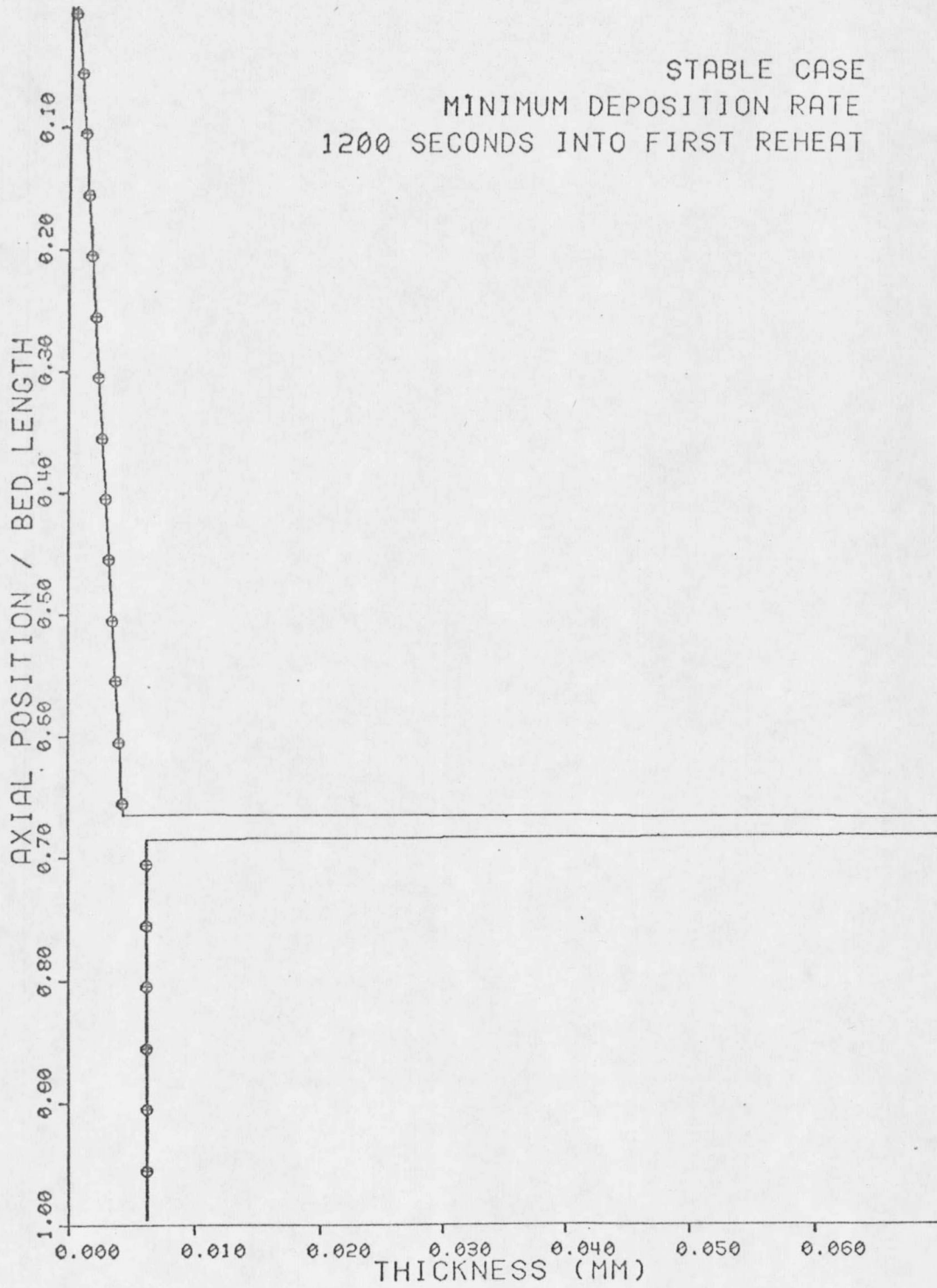


Figure 2.--Seed thickness profile





























































